Quantifying Lateral Solids Mixing in a Fluidized Bed by Modeling the Thermal Tracing Method

Daoyin Liu and Xiaoping Chen
School of Energy and Environment, Southeast University, Nanjing 210096, China

DOI 10.1002/aic.12627
Published online May 6, 2011 in Wiley Online Library (wileyonlinelibrary.com).

Thermal tracing is a simple method for studying solids mixing in fluidized beds. However, the measurement of temperatures is influenced by both mixing and heat transfer, which limits its usefulness for inferring mixing quantitatively. In this work, a semiempirical model is developed to quantify lateral solids mixing in fluidized beds. The model couples the tracer mass balance, the enthalpy balance of tracers and bed particles, and the response dynamic of thermometers. A series of tests is pezrformed in a lab-scale fluidized bed, with particle sizes of 0.28–0.45, 0.45–0.6, 0.6–0.8, and 0.8–1.0 mm, and fluidizing velocity from 0.3 to 2.3 m/s. By evaluating the measured transient temperatures using the model, the lateral dispersion coefficient (D_{sr}) is determined to be between 0.0002 and 0.0024 m^2/s. Its reliability is confirmed by bed collapse experiments. Finally, the values of D_{sr} is compared with a collection of data in the literature. © 2011 American Institute of Chemical Engineers *AIChE J,* 58: 745–755, 2012
Keywords: fluidized bed, solids mixing, dispersion coefficient, thermal tracing method

Introduction

Fluidized bed technology is widely used in physical and chemical processes, e.g., granulation, drying, coating, fluid catalytic cracking, and solid fuel combustion/gasification. The performance of a fluidized bed is highly influenced by the mixing of particles. Solids mixing has thus been a subject of continued interest of study in fluidization engineering since the 1950s (see review articles[1–8]) and has developed into a broad topic. Mixing dynamics in a dense (bubbling/slugging/turbulent) fluidized bed[1,2] are much different from those in a fluidized bed riser.[3] Overall motion characteristics,[1,2] axial mixing,[4] and lateral mixing[5] are also studied using different methods. The overall motion characteristics in a dense bed or a riser can be visualized by tracking an individual radioactive tracer, which provides valuable information that can be used for inferring the mixing rate.[8] Axial mixing in a riser has been studied extensively using a stimulus-response method with various tracers and characterized by residence time distribution.[4,9] The lateral mixing in a riser, although much less investigated, has been effectively studied by phosphor[10] and heated tracing methods.[11,12] These effective methods for investigating mixing in a riser cannot be applied directly in a dense bed study due to much higher solid concentration. In this study, the lateral solids mixing in the dense bed is focused on because the lateral mixing is much less favorable than axial mixing.[1]

Particle tracing methods for lateral solids mixing

Several techniques using a single tracer or a batch of tracers have been developed for measuring solids mixing in the dense zone of fluidized beds. By tracking a single particle continuously, the characteristics of particle motion can be effectively revealed.[13–16] In addition, solid dispersion coefficient can be calculated based on the trajectory.[13,14] More

Correspondence concerning this article should be addressed to X. Chen at xpchen@seu.edu.cn

Table 1. Test Conditions

d_p (mm)	U_0 (m/s)					
0.8–1.0	0.93	1.16	1.33	1.56	1.78	2.22
	A1	A2	A3	A4	A5	A6
0.6–0.8	0.69	0.93	1.22	1.56	1.89	
	B1	B2	B3	B4	B5	
0.45–0.6	0.56	0.79	1.22	1.56	1.89	
	C1	C2	C3	C4	C5	
0.28–0.45	0.32	0.56	0.83	1.16		
	D1	D2	D3	D4		

commonly, the dispersion coefficient is determined by measuring the dispersion of a batch of tracers and modeling using a Fickian-type diffusion equation.[5] The employed tracers include different chemicals (Here, it is classified as Type I tracer),[17,18] different particle sizes (I),[19,20] colored (II),[2,21,22] heated/cooled (III),[23,24] subliming (III),[25,26] reactive to produce gaseous (IV),[5,27] specifically designed porous carbon-loaded (IV),[28] magnetized from a slice of bed particles (V),[29] and radioactive (V)[30] tracers.

Type I experiments obtain tracer mixing directly, but they have to be performed at given intervals, which is both time-consuming and tedious. Type II experiments allow nonintrusive image analysis through which the details of hydrodynamics are also obtained, but they are limited to two-dimensional (2-D) facilities. Type III experiments enable on-line measurements at multiple points simultaneously. They also do not contaminate bed particles, which avoid the separation of tracers. However, the quantitative analysis of measured temperatures is not easy. Type IV techniques are designed to provide convenient methods for solids mixing. They were only developed recently and, to date, their applications are still few. Finally, Type V experiments provide detailed information on particle trajectory, solids flow pattern, etc. They are precious tools in solids mixing study, but their high cost and complexity prohibit their widespread use.

It can be concluded that a convenient, easily implemented, and reliable technique for measuring solids mixing will be attractive. Thermal tracing (Type III tracer) is such a simple approach, but with the referred disadvantages. Valenzuela and Glicksman (1984) used the method for investigating local solids mixing behaviors in a 2-D fluidized bed.[31] Westphalen and Glicksman (1995)[11] and Koenigsdorff and Werther (1995)[12] used it for measuring radial dispersion coefficient in the upper region of a circulating fluidized bed. It is also employed by several other authors for studying solids mixing in fluidized beds.[24,32–35] However, the measured temperatures are influenced by both mixing and heat transfer. To overcome this disadvantage, Westphalen and Glicksman (1995) developed a model, which included energy balance of tracers, bed particles and gas, as well as tracer mass balance, to estimate radial particle diffusivity in the core region of a bed riser, but they could not apply it for solids mixing in the bottom bed.[11]

This study aims to improve the thermal tracing method by building and testing a semiempirical model for analyzing measured temperatures and for quantifying solids mixing in fluidized beds. The present model couples the mass balance of the tracers, the enthalpy balance of the tracers and bed particles, and the thermometer response function. Its overall framework is similar to that developed by Westphalen and Glicksman (1995), but the treatment of tracer feed source, heat transfer source, and thermometer response characteristic are different.

The following sections are arranged as follows: The "Experimental" section gives an essential description of the thermal tracing test. The "Model" section presents the proposed thermal tracing model. Then, the "Results" section presents the evaluated results for a range of operating conditions. In the "Discussion" section, the reliability of the results from the thermal tracing model is compared with the bed collapse tests and a summary of literature data.

Experimental

Experimental conditions

The mixing tests cover a combined range of bed particle size (d_p) and fluidizing velocity (U_0), as listed in Table 1. Several levels of fluidizing velocity are investigated for each of the bed particles. In each test, the bed material comprises 6600 g sand particles and the tracers are heated sand particles whose mass is 1370 g. It is found that 1370 g tracers are enough to enable a repeatable mixing behavior. Too few tracers cannot enable reproducibility of the measurement, and too many tracers would alter the bed hydrodynamics. The minimum fluidization velocities (U_{mf}) for the sand particles with d_p = 0.28–0.45, 0.45–0.6, 0.6–0.8, and 0.8–1.0 mm are experimentally determined to be 0.19, 0.41, 0.60, and 0.69 m/s, respectively.

Apparatus and procedure

The fluidized bed has a cross section of 0.3 m × 0.2 m and a height of 2 m (Figure 1), which is described in detail elsewhere.[19] It is equipped with tracer feed and detection components. A tracer container with a feed tube is located at the sidewall. The feed tube, with an inner diameter of 38 mm, connects the bed at a height of 0.15 m above the distributor. A ball valve is installed in the feed tube. In each test, when the bed has reached steady-state fluidization, the tracers are poured into the container. Then at one moment,

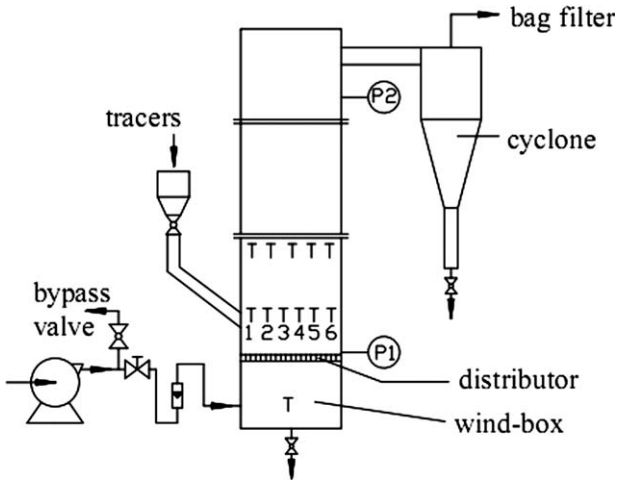

Figure 1. Schematic diagram of fluidized bed apparatus.

The bed has a rectangular cross section of 0.3 m × 0.2 m and a height of 2 m.

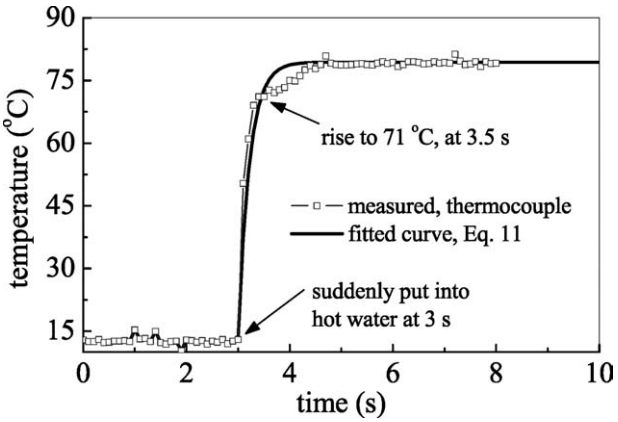

Figure 2. Response characteristic of the thermocouple.

The thermocouple is suddenly placed from air into hot water.

the valve is opened quickly, the tracers flow into the bed, and then mix with the bed particles. The tracers can flow into the bed by gravity because the feed port is located in the splashed zone above the bed surface. The pressure drop between the two points P1 and P2 in Figure 1 is monitored to reflect the tracer injection process. It is found from the pressure drop measurement that the feeding duration is approximately 4–5 s.

The tracers are prepared using the following steps. First, a batch of weighed tracers is heated to 100°C in an oven. Then the tracers are kept in the oven for another 30 mins, which enables the particles to reach thermal equilibrium. Next, the tracers are quickly poured into the tracer container kept warm by a heater band. Finally, the tracers are fed into the bed at one moment. Note that the present tracer preparation method cannot ensure the tracers are at exactly 100°C. Heat balance calculation, using Eq. 13 below, shows that the tracer temperatures in different tests are in the range of 90–103°C. Tracer temperature can be influenced by the final tracer temperature in the oven, the process of transferring tracers from the oven to the container, and the period when the tracers in the container are waiting for feeding. In the modeling below, the calculated temperature using Eq. 13 is used as the input of the tracer temperature instead of 100°C. In further studies of thermal tracing tests, it is better to seek other ways for preparing heated tracers, such as using a fluidized device to heat and feed tracers.

A group of thermocouples indicated in Figure 1 are used to monitor local temperatures. One thermocouple monitors the temperature below the distributor. Six thermocouples, denoted as Nos. 1 to 6, are arranged in a line at a height of 0.07 m above the gas distributor to monitor lateral temperature profiles in the dense bed. Another five monitor temperatures at a height away from the dense bed. The employed thermocouple is naked, with a point head of 1.1 mm diameter, ensuring quick response to the transient temperature. Figure 2 illustrates its response characteristic: the thermocouple reaches 90% of the change within 0.5 s when it is suddenly moved from air into hot water. The heat-transfer coefficient at the thermocouple in water is different from that in fluidized beds; thus, it is incorporated into the thermocouple response function as described in the "Model" section. Another kind of thermometer, a PN thermistor, which shows a slower response, is tested, as given in the "Discussion" section.

Model

The objective is to quantify lateral solids mixing in a fluidized bed by modeling the coupled effects of mixing, heat transfer, and transient temperature measurement errors. Figure 3 depicts the overall model framework, taking into account the mass balance of the tracers, the enthalpy balance of the tracers and bed particles, and the thermometer response characteristic. Assigning a value for the lateral solids dispersion coefficient (D_{sr}) the model predicts a spatio-temporal temperature distribution, which is then compared with the measured temperatures.

Simplifications

Many of the published works employ a Fickian-type diffusion equation to fit the complex lateral mixing process,[5] In this method, mixing induced by different factors, such as local bubble movement and gross emulsion circulation, is lumped into an effective dispersion coefficient. The present model adopts the diffusion equation for tracer mass dispersion. Vertical mixing of solids is preferred over lateral mixing because the motion of bubbles is promoted in a vertical direction.[1] Experimental investigations concerning solids mixing in the fluidized bed bottom zone reveal a uniform vertical tracer distribution.[25] Thus, in the model below, the tracers are assumed to be vertically uniform.

Tracer mass balance

Solids mixing in the bottom zone (including dense bed and splashed zone) is modeled, and the modeling geometry is shown in Figure 4. Tracer mass concentration is defined as $C_t \equiv m/A$ [kg tracers/m^2 cross-section area], which represents tracer mass per cross-section area. Almost no elutriation of particles was observed due to narrow particle-size distribution. Its conservation can be described by the 2-D dispersion equation:

$$\frac{\partial C_t}{\partial t} = D_{sr}\left(\frac{\partial^2 C_t}{\partial x^2} + \frac{\partial^2 C_t}{\partial y^2}\right) + S_{feed} \tag{1}$$

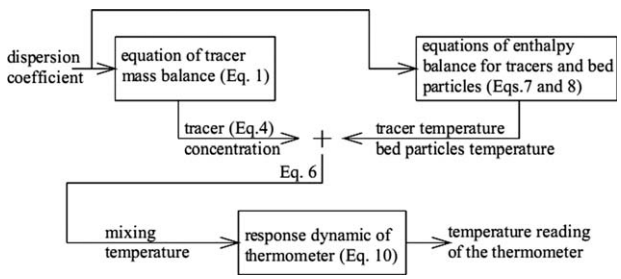

Figure 3. Overall framework of the developed model.

Assigning a value for dispersion coefficient in the model, it predicts a spatio-temporal temperature distribution which can be directly compared with the measured temperatures.

where D_{sr} is the effective dispersion coefficient and S_{feed} is the tracer mass source. In the model, it is assumed that there is an initial distribution of the tracer feed around the feed point (A_{feed}). S_{feed} is zero outside A_{feed}, whereas within A_{feed}, it is determined by

$$S_{feed} = \begin{cases} M_{feed}/(A_{feed}t_{feed}) & t \le t_{feed} \\ 0 & t > t_{feed} \end{cases} \quad (2)$$

where M_{feed} is the tracer mass and t_{feed} is the tracer feed duration. According to the experimental condition, the value of M_{feed} is 1370 g and that of t_{feed} is 5 s. However, the value of A_{feed} has to be assumed. A_{feed} is assumed to be 4 cm $\times$ 5 cm around the feed point. During preprimary calculations no evident difference in temperature predictions is observed, as A_{feed} is changed within a reasonable range.

With the following initial and boundary conditions:

$$\begin{aligned} &t = 0,\ C_t = 0 \\ &t > 0,\ \left.\frac{\partial C_t}{\partial x}\right|_{x=0,L} = \left.\frac{\partial C_t}{\partial y}\right|_{y=0,B} = 0 \end{aligned} \quad (3)$$

Equation 1 yields a transient distribution of the tracer mass concentration, C_t. It is converted to a nondimensional parameter:

$$\eta = \frac{C_t}{C_t + C_b} \quad (4)$$

where C_b is the mass concentration of bed particles, and η is the local tracer mass fraction.

Mixing temperature

Given a local volume in the dense bed, which contains tracer particles, bed particles, and gas, local temperature can be calculated as

$$T_{mix} = \frac{c_{ps}m_tT_s + c_{ps}m_bT_b + c_{pg}m_gT_g}{c_{ps}m_t + c_{ps}m_b + c_{pg}m_g} \quad (5)$$

Since the gas density is smaller than particle density by three orders of magnitude, the contribution of gas to T_{mix} is negligible

$$T_{mix} = \frac{m_tT_t + m_bT_b}{m_t + m_b} = \eta T_t + (1-\eta)T_b \quad (6)$$

According to Eq. 6, T_t and T_b, as well as η, should be known for predicting T_{mix}. Therefore, the enthalpy balance of the tracers and the bed particles are built to obtain T_t and T_b, respectively.

Enthalpy balance

Enthalpy concentration of the tracers is defined as $H_t = C_tc_{ps}T_t$ [J/m^2 cross-section area], which represents the tracer enthalpy per cross-section area. It is balanced by the accumulated term, the heat transported with the tracer dispersion, and the heat transferred from the fluidizing gas and bed particles:

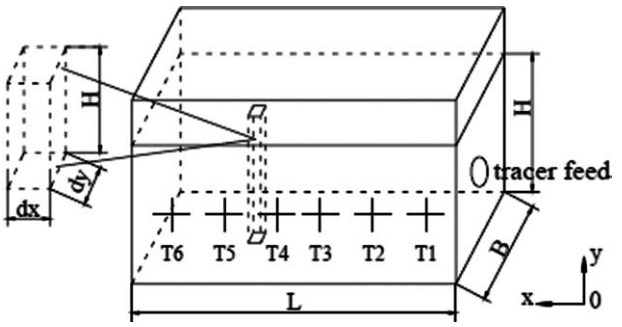

Figure 4. Modeling geometry.

The tracers are assumed to be uniform in the vertical direction.

$$\begin{aligned} &\frac{\partial H_t}{\partial t} = D_{sr}\left(\frac{\partial^2 H_t}{\partial x^2} + \frac{\partial^2 H_t}{\partial y^2}\right) + S_{H,feed} + S_{gt} + S_{bt} \\ &t = 0, H_t = 0 \\ &t > 0,\ \left.\frac{\partial H_t}{\partial x}\right|_{x=0,L} = \left.\frac{\partial H_t}{\partial y}\right|_{y=0,B} = 0 \end{aligned} \quad (7)$$

where $S_{H,feed}$ ($=S_{feed}c_{ps}T_t$) is the enthalpy source due to the tracer feed, S_{gt} is the heat transfer from the gas to the tracers, and S_{bt} is the heat transfer from the bed particles to the tracers.

Similarly, enthalpy concentration of the bed particles is defined as $H_b = C_bc_{ps}T_b$ [J/m^2 cross-section area]. Its conservation equation is

$$\begin{aligned} &\frac{\partial H_b}{\partial t} = D_{sr}\left(\frac{\partial^2 H_b}{\partial x^2} + \frac{\partial^2 H_b}{\partial y^2}\right) + S_{gb} + S_{tb} \\ &t = 0, H_b = C_bc_{ps}T_{b0} \\ &t > 0,\ \left.\frac{\partial H_b}{\partial x}\right|_{x=0,L} = \left.\frac{\partial H_b}{\partial y}\right|_{y=0,B} = 0 \end{aligned} \quad (8)$$

where S_{gb} is the heat transfer from the gas to the bed particles, and S_{tb} ($=-S_{bt}$) is the heat transfer from the tracers to the bed particles.

The source terms of S_{gt}, S_{bt}, and S_{gb} in Eqs. 7 and 8 are calculated by a similar method. S_{gb}, for example, is determined by the limiting values of

$$S_{gb} = \min\left(\frac{6\varepsilon_s H}{d_p}h_{gb}\Delta T_{gb}, \rho_g U_0 c_{pg}(T_{g0} - T_{eq})\right) \quad (9)$$

where the first term on the right-hand side is the convective heat transfer between the gas and the particles, and the second term is determined by assuming a local thermal equilibrium. The parameter of $6\varepsilon_sH/d_p$ represents the heat transfer surface area per unit volume shown in Figure 4.

Thermometer response characteristic

Thermometer readings can deviate somewhat from the actual transient change of T_{mix} because it takes time for the thermometer to develop a response. According to the unsteady heat conduction theory, the thermometer response characteristic can be described by the following equation:

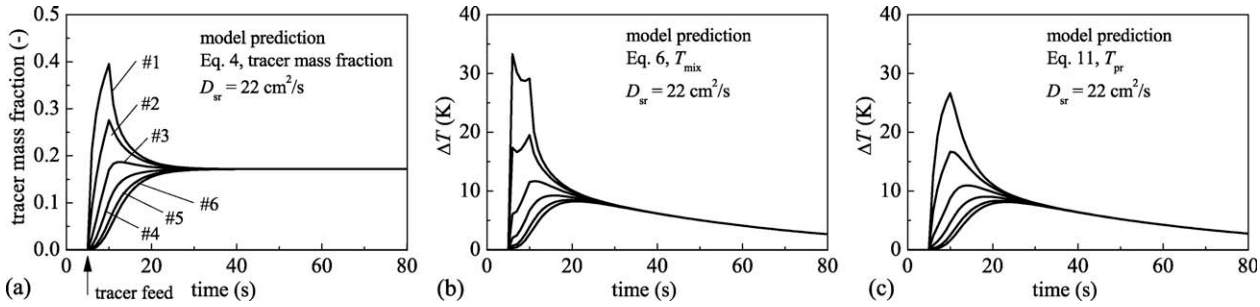

Figure 5. Model prediction of (a) tracer mass fraction, (b) mixing temperature and (c) thermometer reading.

$D_{sr} = 22$ cm^2/s, at the monitors from Nos. 1 to 6.

$$\frac{dT_{pr}}{d\tau} = -\frac{A_p}{\rho_p c_p V_p} h_{pf}\left(T_{pr} - T_\infty\right) \tag{10}$$

where T_{pr} is the thermocouple reading, T_∞ is the actual temperature of the surrounding environment, and h_{pf} is the heat-transfer coefficient between thermocouple and surrounding environment. The combined parameters of $A_p/\rho_p c_p V_p$, which are physical properties of the thermometer, are constant.

Given the response test for the naked thermocouple (Figure 2), with $Nu_p = 2$ in still water, by fitting the solution of Eq. 10 with the thermocouple's reading, the value of $A_p/\rho_p c_p V_p$ is obtained. Thus, the thermocouple response characteristic is

$$\frac{dT_{pr}}{d\tau} = -0.004 h_{pf}\left(T_{pr} - T_\infty\right) \tag{11}$$

In the modeling of thermal tracing test, T_∞ represents T_{mix} from Eq. 6, and h_{pf} is calculated by

$$Nu_p = 2 + (0.6 - 1.8) Re_p^{0.5} \mathrm{Pr}^{0.333} \tag{12}$$

where the coefficient of the second term in the right-hand side is assigned as 1.2 in the present simulation based on the recent experimental studies.[36]

Initial temperatures of the tracers

As described in the "Experimental" section, the present tracer preparation method cannot ensure the tracers are exactly at 100°C. Initial tracer temperature is determined by heat balance calculation instead of being set as 100°C. It is calculated according to the bed temperature at time t and heat loss

$$T_{t,0} = \frac{1}{c_{ps} M_t} \left(\begin{array}{l} c_{ps} T_{b,t} M_b + c_{ps} T_{b,t} M_t - c_{ps} T_{b,0} M_b \\ + c_{pg} \rho_g u_g A_{bed} \int_0^t \Delta T_g \, d\tau \end{array} \right) \tag{13}$$

where $T_{t,0}$ and $T_{b,0}$ are the initial temperatures of the tracers and the bed particles, $T_{b,t}$ is the bed temperature at time t, and ΔT_g is the gas temperature rise when going through the bed. Heat balance calculations show that the tracer temperatures in different tests are in the range of 90–103°C.

Calculation procedure

Given a value for D_{sr}, Eqs. 1, 7, and 8, a system of partial different equations, are solved iteratively using the finite volume algorithm.[37] Applying their results, η, T_t, and T_b, into Eq. 6 yields the mixing temperature, T_{mix}. Placing T_{mix} into Eq. 11, an ordinary differential equation, simulates the dynamic response of the thermometers, T_{pr}. Then, T_{pr} at monitors Nos.1 to 6 are compared with the measured results at one mixing time, where the parameter root mean square error (RMSE) is introduced to help select a time at which the comparison of prediction with measurement is made. RMSE is defined as

$$\mathrm{RMSE}_t = \sqrt{\sum \left(T_{i,t} - T_{ave,t}\right)/N} \tag{14}$$

where $T_{i,t}$ is the temperature response of monitor i at time t, N is the number of monitors, and $T_{ave,t}$ is the average temperature response of the N monitors. During calculation, three mixing times, corresponding to RMSE at 2.5, 3.5, and 4.5 K, respectively, are selected for comparison of prediction with measurement.

Results

An illustrative example of model comparison with experiment

Figure 5 illustrates an example of the model prediction. Given $D_{sr} = 22$ cm^2/s, the model sequentially predicts the transient behaviors of tracer mass fractions (η), mixing temperature (T_{mix}), and thermometer reading (T_{pr}), as shown in Figures 5a–c, respectively. The variation of η shows a clear mixing process. After about 25 s, η at different positions reaches equilibrium and remains constant. The variation of T_{mix} is similar to that of η, but one difference is that T_{mix} decreases constantly with time because the heat of bed materials is transferred to the fluidizing gas and carried away continuously. The variation of T_{pr}, which includes the lag of thermometer response, is very close to that of T_{mix} because the employed thermometer has a quick response.

Although η is a direct measure of tracer dispersion, it is not easy to measure. In contrast, T_{pr}, although an indirect measure of tracer dispersion, can be measured conveniently using the thermal tracing test. Figure 6 compares T_{pr}, predicted by the model with $D_{sr} = 22$ cm^2/s, with the measured temperatures at Test B5 ($d_p = 0.6$–0.8 mm, $U_0 = 1.89$ m/s). Two calculations using the model are performed to demonstrate the influence of heat transfer. One calculation is performed without heat transfer, assuming that the heat source

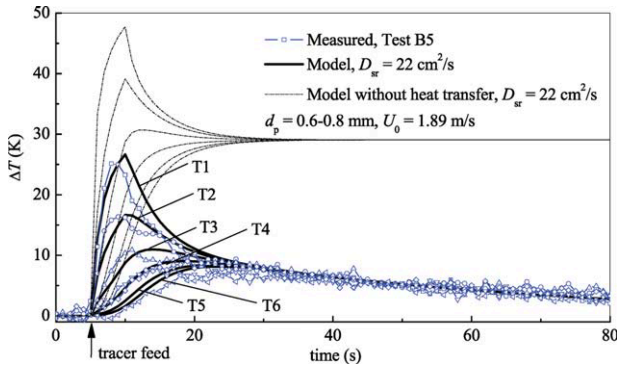

Figure 6. Comparison of model prediction with D_{sr} = 22 cm^2/s, with measurement at Test B5 (d_p = 0.6–0.8 mm, U_0 = 1.89 m/s).

The model prediction with heat transfer effect (solid lines) and without heat transfer effect (dash lines) are compared. [Color figure can be viewed in the online issue, which is available at wileyonlinelibrary.com.]

terms of S_{gt}, S_{bt}, and S_{gb} in Eqs. 7 and 8 are zero, and the heat transfer in the other calculation is normal. A reasonable agreement between the measured temperatures and the prediction with heat transfer is noted, but the calculation without heat transfer gives an incorrect prediction of the temperature.

Lateral solids dispersion coefficient

Figure 7 compares the measured and calculated temperature responses at different lateral positions for different fluidizing velocities and constant particle size. In each figure, the calculated temperature profiles are plotted as solid lines and the calculated value of D_{sr} is indicated. The general behavior of the computed temperature is consistent with the measurement. By increasing fluidizing velocity from 0.69 to 1.56 m/s, temperature equilibrium is achieved faster and, as expected, the determined value of D_{sr} is increased from 2 to 15 cm^2/s. As fluidizing velocity is increased, the bubble dynamics become more vigorous, which promote solids mixing.

The calculated and measured temperatures are generally in agreement, except for the first few seconds after the tracer feed. Note that the prediction of the monitors at Nos. 1 and 2, which are closer to the feed point, is lower than the measurement, indicating an overprediction of the tracer dispersion. Some calculations performed by Liu and Chen (2010)[19] assume smaller values of D_{sr} near the bed wall and larger ones in the bed core region, yielding a very good agreement between calculated and measured temperatures. However, a constant value of D_{sr} is assumed upon calculation, which is more practical and common in literature. Furthermore, the above mentioned disagreement disappears gradually with time. Given enough seconds for mixing, it is acceptable to simplify lateral mixing by assuming a constant value of D_{sr} in the dispersion model. Actually, in the studies by Winaya et al. (2007)[28] and Liu and Chen (2010),[19] by assuming a constant value of D_{sr} in the dispersion model, the disagreement is also noted at the beginning of mixing between measured transient tracer profiles and dispersion model.

The tests are also performed for d_p = 0.28–0.45, 0.45–0.6, and 0.8–1.0 mm under different fluidizing velocities. In each test, the measured transient temperature profiles are compared with model predictions, yielding a value of D_{sr}. The results are not shown individually because they are similar to those presented in Figure 7.

Figure 8 shows the RMSE of the transient temperature profiles, defined by Eq. 14, as a function of time for all the tests performed with different particle sizes. RMSE, the deviation of temperature distribution, can indicate the mixing process. A reasonable agreement between calculated and measured RMSE can be seen for each test, except that the disagreement at the beginning of the tracer feed which has a limited influence on the overall prediction. Therefore, such a

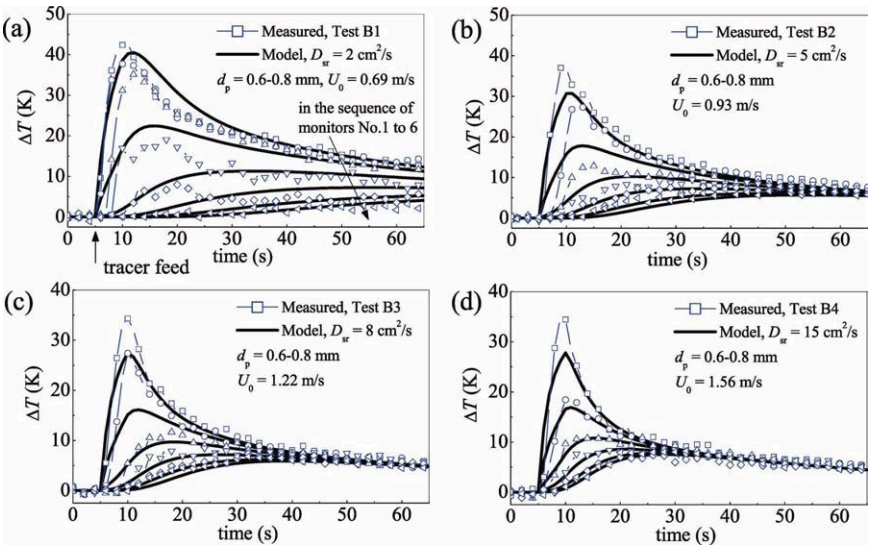

Figure 7. Measured (symbols) and calculated (lines) temperature responses at the monitors from Nos.1 to 6 for different fluidizing velocities with d_p = 0.6–0.8 mm.

(a) U_0 = 0.69 m/s; (b) U_0 = 0.93 m/s; (c) U_0 = 1.22 m/s; (d) U_0 = 1.56 m/s. In each figure the value of D_{sr} is indicated. [Color figure can be viewed in the online issue, which is available at wileyonlinelibrary.com.]

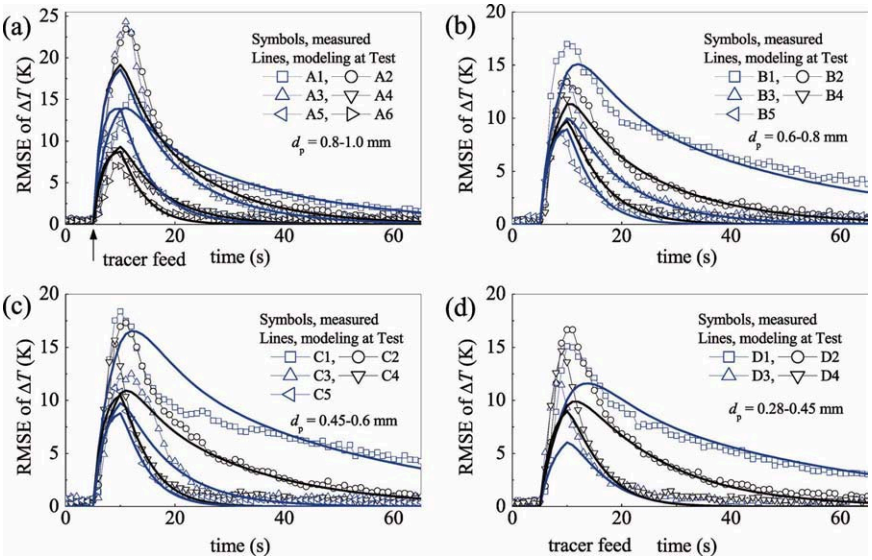

Figure 8. RMSE of measured (symbols) and calculated (lines) temperature responses for all the tests listed in Table 1.

(a) d_p = 0.8–1.0 mm; (b) d_p = 0.6–0.8 mm; (c) d_p = 0.45–0.6 mm; (d) d_p = 0.28–0.45 mm. [Color figure can be viewed in the online issue, which is available at wileyonlinelibrary.com.]

model is capable of modeling the overall behaviors of the thermal tracing test. Figure 9 summarizes D_{sr} as a function of the fluidizing velocity for each bed material. For each test, the average value of D_{sr} had error bars which resulted from computing D_{sr} at three mixing times, corresponding to the RMSE of 2.5, 3.5, and 4.5 K, respectively. The values of D_{sr} lie in the range of 0.0002–0.0024 m^2/s. The obtained D_{sr} is compared with literature data in the following section.

Discussion

Influence of thermometer response speed

Before discussing D_{sr} further, let us check the influence of thermometer response speed. Figure 10 compares the response speed of the two types of thermometers: the naked thermocouple (TC) whose response characteristic is illustrated in Figure 2, and the PN thermistor (PNT). As shown in Figure 10, PNT develops a slower response compared to TC, and its response characteristic is described by

$$\frac{dT_{pr}}{d\tau} = -0.0022 h_{pf}\left(T_{pr} - T_{\infty}\right) \tag{15}$$

Figure 11 compares the measurements by TC and PNT for two tests. At the monitor of No. 1, where temperatures change rapidly, the reading from the PNT is obviously smaller than that from the TC, but they coincide with each other after a few seconds where the changes are slower. It can be inferred that the thermometer would not capture the transient temperatures if its response is further slower. Therefore, it is very critical to use the quick response thermometer to ensure a reliable tracing

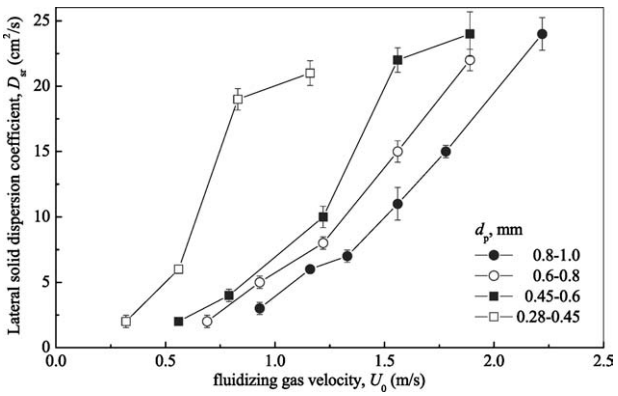

Figure 9. Lateral solids dispersion coefficient (D_{sr}) as a function of fluidizing velocity for all the tests listed in Table 1.

For each test, the averaged value of D_{sr} is reported with error bars. The error bars result from computing D_{sr} at three mixing times, corresponding to RMSE of 2.5, 3.5, and 4.5 K, respectively.

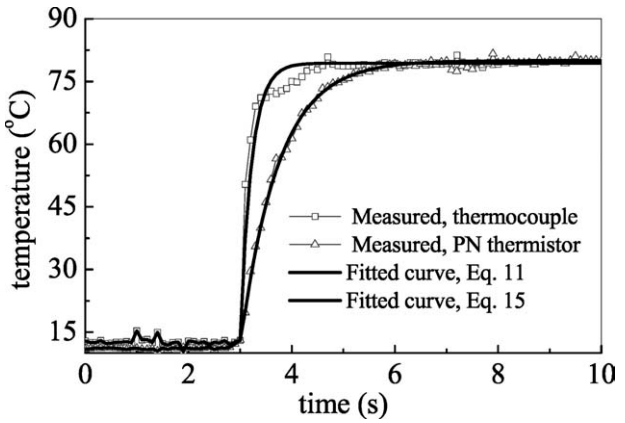

Figure 10. Comparison of response characteristic for the thermocouple and PN thermistor.

They are suddenly placed from air into hot water.

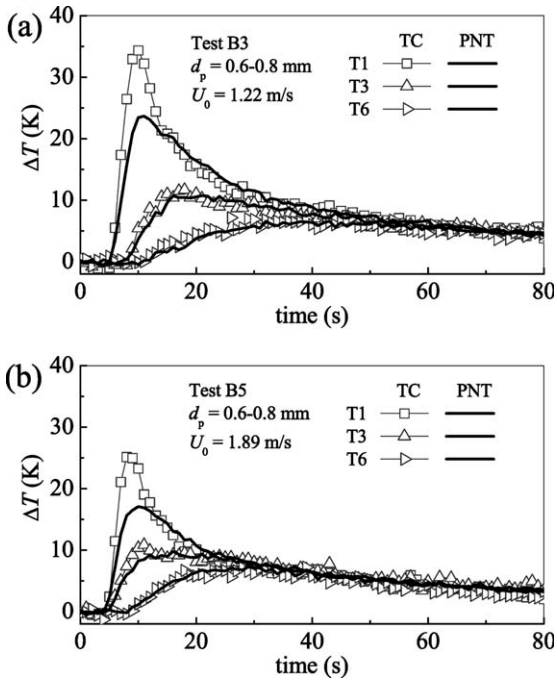

Figure 11. Comparison of thermal tracing measurements by thermocouples (TC) and PN thermistors (PNT) at the monitors of Nos.1, 3, and 6.

(a) $d_p = 0.6$–0.8 mm, $U_0 = 1.22$ m/s; (b) $d_p = 0.6$–0.8 mm, $U_0 = 1.89$ m/s.

measurement. It is noted in the study by Glicksman et al. (2008) that they used thermistors with very fast response, which enabled the investigation of particle injection and mixing behaviors in a fluidized bed.[24]

Comparison with the bed collapse method

Liu and Chen (2010) obtained spatio-temporal lateral mixing behaviors by the bed collapse method with a novel sampling tool, and thermal tracing measurements with the PN thermistors.[19] A preliminary comparison of the thermal tracing measurements with the bed collapse measurements is given by them. Here, a further comparison is made. Figure 12

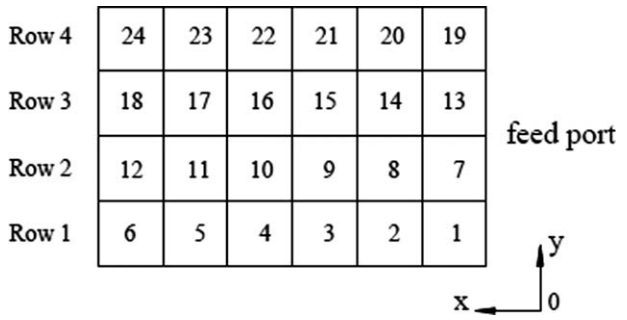

Figure 12. Top view and index of the 24 sample cells.

They are used for comparison tests of thermal tracing method with bed collapse method.

shows the layout of the 24 sample cells in the bed cross section. The bed collapse measurements, at the conditions of (1) $U_0 = 0.6$ m/s and (2) $U_0 = 1.2$ m/s, with bed particles $d_p = 0.28$–0.45 mm and tracers $d_t = 0.8$–1.0 mm, can be referred to Figures 7 and 8 in the previous paper.[19] Figure 13 shows the measured transient temperature profiles, for the corresponding conditions, at the positions of the 24 sample cells. Maximal temperature rise decreases along the X direction but remains similar along the Y direction, which is consistent with the 2-D lateral tracer concentration profiles.[19] By increasing U_0 from 0.6 to 1.2 m/s, the response becomes more rapid as expected, indicating an improvement in tracer dispersion.

Furthermore, the 2-D lateral tracer concentration profiles at different mixing times, in Figures 7 and 8 of the previous study,[19] and the transient temperatures at different lateral positions, in Figure 13 of this article, are evaluated using the model developed in this work. Figures 14 and 15 present the evaluated results for $U_0 = 0.6$ m/s and $U_0 = 1.2$ m/s, respectively. In Figure 14a, a comparison is made for the tracer mass fraction, with symbols representing the data obtained by bed collapse measurements and lines predicted by Eq. 1 with $D_{sr} = 5$ cm^2/s. Similarly, in Figure 14b, a comparison is made for the temperature, both predicted and measured by thermal tracing tests, with $D_{sr} = 7$ cm^2/s. The agreement between model and measurement is reasonable. For $U_0 = 1.2$ m/s, shown in Figure 15, the D_{sr} is determined to be

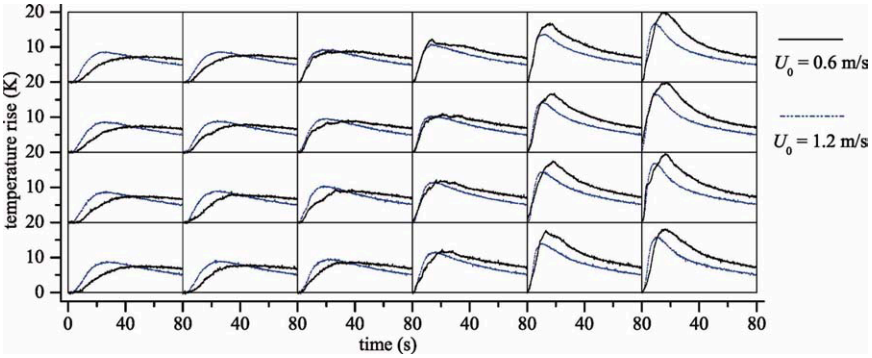

Figure 13. Transient temperature response at the positions corresponding to the 24 sample cells.

(a) $U_0 = 0.6$ m/s and (b) $U_0 = 1.2$ m/s, with $d_p = 0.28$–0.45 mm and $d_t = 0.8$–1.0 mm. [Color figure can be viewed in the online issue, which is available at wileyonlinelibrary.com.]

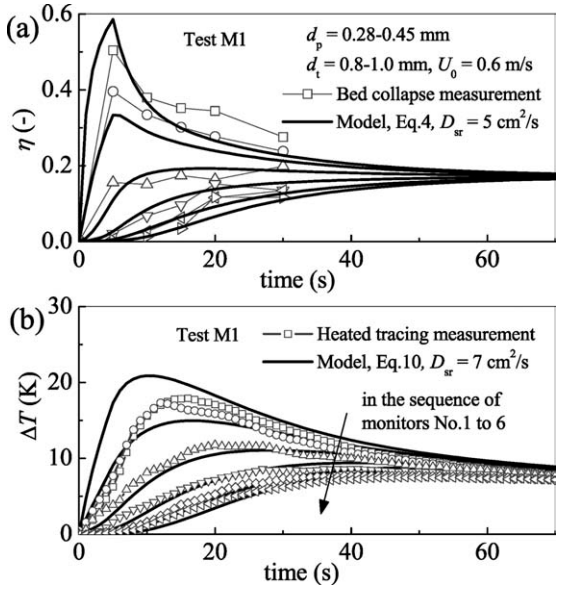

Figure 14. Model evaluation of two tracing methods.

(a) comparison of bed collapse measurement and model evaluation; (b) comparison of thermal tracing measurement and model evaluation. U_0 = 0.6 m/s, d_p = 0.28–0.45 mm and d_t = 0.8–1.0 mm, at the monitors from Nos. 1 to 6.

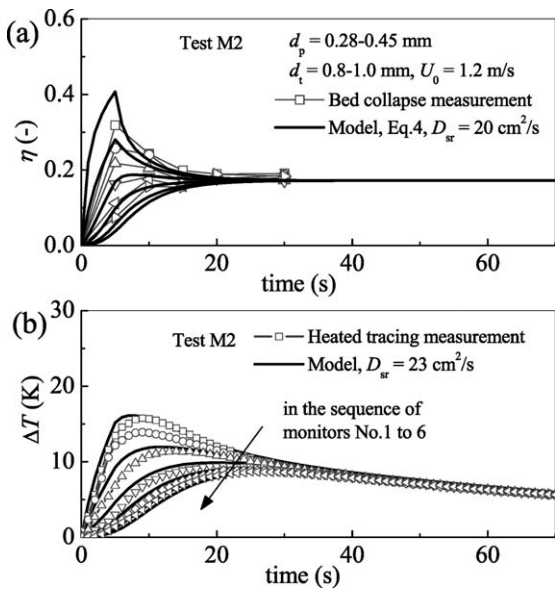

Figure 15. Model evaluation of two tracing methods.

(a) comparison of bed collapse measurement and model evaluation; (b) comparison of thermal tracing measurement and model evaluation. U_0 = 1.2 m/s, d_p = 0.28–0.45 mm and d_t = 0.8–1.0 mm, at the monitors from Nos. 1 to 6.

20 cm^2/s and 23 cm^2/s using the two methods. Therefore, the determined values of D_{sr} by the two methods are consistent, leading to the conclusion that the improved thermal tracing method in this article is reliable for measuring lateral solids dispersion coefficient quantitatively. The key point is that the temperature can be measured more conveniently than the tracer concentration.

Comparison with literature data

Many studies have been carried out for measuring lateral solids mixing in the fluidized bed bottom zone. Figure 16 presents a compilation of D_{sr} reported in the literature after the 1980s. Each line in Figure 16a, with D_{sr} plotted against U_0–U_{mf}, is from a separate set of experiments, with its conditions noted in the right of Figure 16. For better clarity, the average

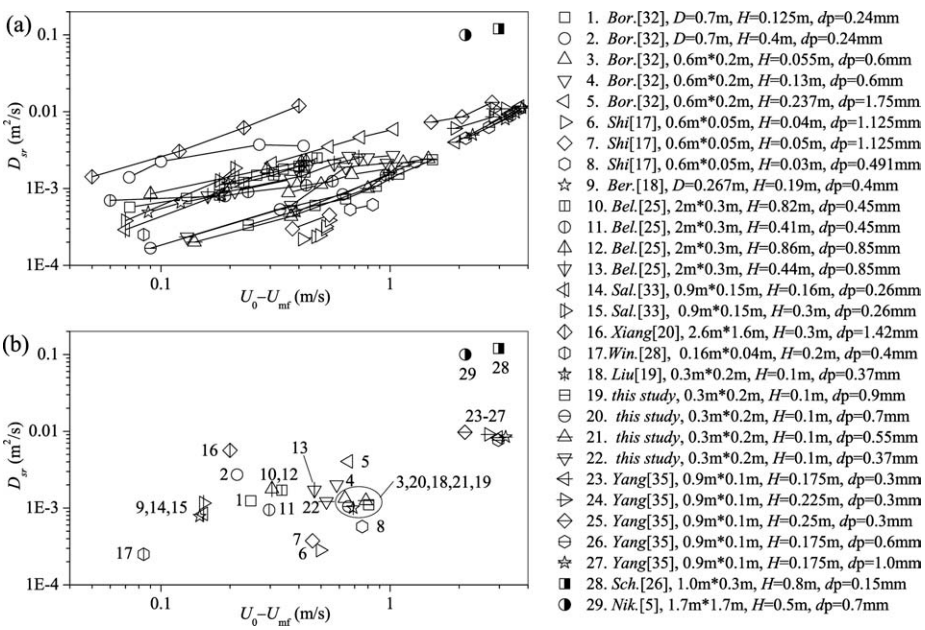

Figure 16. A compilation of lateral solids dispersion coefficient (D_{sr}) reported in the literature after the 1980s.

The data cover a wide range of bed size, fluidizing velocity, static bed height, and particle size. (a) each line plots D_{sr} against $U_0 - U_{mf}$; (b) each data point is calculated by averaging each line in (a).

of each line is calculated, which yielded the data in Figure 16b. The reviewed data cover a wide range of bed size, fluidizing velocity, bed height, and particle size. It shows that D_{sr} is scattered from 0.0001 to 0.1 m^2/s. There are only two data points around 0.1 m^2/s, which are obtained in pilot fluidized beds at higher fluidizing velocities.[5,26] A few points are around 0.01 m^2/s.[20,32,35] An example in this group is that of Yang et al., who measured D_{sr} in the bottom zone of a CFB with a width of 0.9 m.[35] Most of the other data, obtained either in smaller facilities or at lower fluidizing velocities, fall at $\sim$0.001 m^2/s. The D_{sr} obtained in this study falls into this group. Therefore, a strong dependence of D_{sr} on bed size and fluidizing velocity is established, although parts of the scatter are due to experimental techniques and data analysis. More detailed investigations on solids mixing using advanced experimental techniques and numerical simulations are still required in the future study.

Conclusions

This article presents a semiempirical thermal tracing model for quantifying lateral solids mixing in dense fluidized beds. The model includes tracer mass balance based on the widely used Fickian-type diffusion equation, enthalpy balance of tracers and bed particles, and thermometer response characteristic, to describe the coupled effects of mixing, heat transfer, and dynamic measurement errors. Assigning a value of the lateral dispersion coefficient (D_{sr}) in the model, it predicts a spatio-temporal temperature distribution, which can be compared directly with measured temperatures from the thermal tracing experiment.

The model is employed to evaluate a series of tests performed in a lab-scale fluidized bed, with particle sizes of 0.28–0.45, 0.45–0.6, 0.6–0.8, and 0.8–1.0 mm, and fluidizing velocity from 0.3 to 2.3 m/s. The D_{sr} is determined to be between 0.0002 and 0.0024 m^2/s. By comparing the results from thermal tracing and bed collapse experiments, the reliability of the thermal tracing method is confirmed. Finally, results are compared with literature data.

There is a lack of easily implemented and reliable methods for investigating solids mixing quantitatively in dense fluidized beds. The improved thermal tracing method, presented in this article with a detailed discussion on its implementation, measurement, data treatment, and validation, is a good choice for measuring the mixing rate of solids.

Acknowledgments

Financial supports of this work by the High-tech Research and Development Program of China (2009AA05Z311) and the Scientific Research Foundation of Graduate School of Southeast University are gratefully acknowledged. The authors thank the anonymous Reviewers of this manuscript for their insightful and detailed comments.

Notation

A_{feed} = an assumed initial distribution of the tracer around the feed point, m^2
$A_p/\rho_p c_p V_p$ = surface area/(density × specific heat capacity × volume) of the thermometer head, in Eq. 10, m^2 K)/J
C_b = mass concentration of the tracer particles per cross section area, kg/m^2
C_t = mass concentration of the bed particles per cross section area, kg/m^2
c_p = specific heat capacity, J/(kg K)
D_{sr} = lateral solids dispersion coefficient, m^2/s
d = particle diameter, mm
H_b = enthalpy concentration of the bed articles per cross section area, J/m^2
H_t = enthalpy concentration of the tracer particles per cross section area, J/m^2
h_{pf} = heat-transfer coefficient between the thermometer and fluid, $W/(m^2K)$
M_{feed} = tracer mass, kg
m = mass, kg
Nu = Nusselt number, dimensionless
Pr = Prandtl number, dimensionless
Re = Reynolds number, dimensionless
S_{feed} = tracer mass source, $kg/(m^2s)$
$S_{H,feed}$ = enthalpy source due to the tracer feed, $J/(m^2\ s)$
S_{gt} = enthalpy source due to heat transfer from the gas to tracers, $J/(m^2\ s)$
S_{bt} = enthalpy source due to heat transfer from the bed particles to tracers, $J/(m^2\ s)$
S_{tb} = $-S_{bt}$, $J/(m^2\ s)$
S_{gb} = enthalpy source due to heat transfer from the gas to bed particles, $J/(m^2\ s)$
t_{feed} = tracer feed duration, s
T = temperature, K
T_{pr} = thermocouple's reading, in Eq. 10, K
T_∞ = actual temperature of the fluid, in Eq. 10, K
$T_{t,0}$ = initial temperature of the tracers, in Eq. 13, K
$T_{b,0}$ = initial temperature of the bed particles, in Eq. 13, K
$T_{b,t}$ = temperature of the bed particles at time t, in Eq. 13, K
T_{eq} = thermal equilibrium temperature in a unit volume, K
ΔT = temperature difference, K
U_0 = fluidizing gas velocity, m/s
U_{mf} = minimal fluidization velocity, m/s
x = x–direction, m
y = y–direction, m

Greek letters

τ = time, s
ρ = density, kg/m^3
ε = voidage, dimensionless
ε_s = solid volume fraction, dimensionless
η = tracer mass fraction, dimensionless

Subscripts

b = bed particle
f = fluid
g = gas
mf = minimal fluidization
mix = mixture of tracers, bed particles, and gas
p = particle
s = solid
t = tracer

Literature Cited

1. Kunii D, Levenspiel O. *Fluidization Engineering*, 2nd ed. Boston: Butterworth-Heinemann Press, 1991.
2. Lim KS, Gururajan VS, Agarwal PK. Mixing of homogeneous solids in bubbling fluidized-beds—theoretical modeling and experimental investigation using digital image-analysis. *Chem Eng Sci*. 1993; 48:2251–2265.
3. Werther J, Hirschberg B. *Solids motion and mixing*. In: Grace JR, Avidan AA, Knowlton TT, editors. *Circulating Fluidized Beds*. London: Blackie Academic & Professional, 1996:119–148.
4. Harris AT, Davidson JF, Thorpe RB. A novel method for measuring the residence time distribution in short time scale particulate systems. *Chem Eng J*. 2002;89:127–142.
5. Niklasson F, Thunman H, Johnsson F, Leckner B. Estimation of solids mixing in a fluidized-bed combustor. *Ind Eng Chem Res*. 2002; 41:4663–4673.

6. Breault RW. A review of gas-solid dispersion and mass transfer coefficient correlations in circulating fluidized beds. *Powder Technol*. 2006;163:9–17.
7. Mohs G, Gryczka O, Heinrich S, Morl L. Magnetic monitoring of a single particle in a prismatic spouted bed. *Chem Eng Sci*. 2009; 64:4811–4825.
8. Chan CW, Seville JPK, Parker DJ, Baeyens J. Particle velocities and their residence time distribution in the riser of a CFB. *Powder Technol*. 2010;203:187–197.
9. Rhodes MJ, Zhou S, Hirama T, Cheng H. Effects of operating-conditions on longitudinal solids mixing in a circulating fluidized-bed riser. *AIChE J*. 1991;37:1450–1458.
10. Du B, Fan LS, Wei F, Warsito W. Gas and solids mixing in a turbulent fluidized bed. *AIChE J*. 2002;48:1896–1909.
11. Westphalen D, Glicksman L. Lateral solid mixing measurements in circulating fluidized beds. *Powder Technol*. 1995;82:153–167.
12. Koenigsdorff R, Werther J. Gas-solids mixing and flow structure modeling of the upper dilute zone of a circulating fluidized bed. *Powder Technol*. 1995;82:317–329.
13. Mostoufi N, Chaouki J. Local solid mixing in gas-solid fluidized beds. *Powder Technol*. 2001;114:23–31.
14. Pallarès D, Johnsson F. A novel technique for particle tracking in cold 2-dimensional fluidized beds—simulating fuel dispersion. *Chem Eng Sci*. 2006;61:2710–2720.
15. Wong YS, Seville JPK. Single-particle motion and heat transfer in fluidized beds. *AIChE J*. 2006;52:4099–4109.
16. Yang Z, Fan X, Fryer PJ, Parker DJ, Bakalis S. Improved multiple-particle tracking for studying flows in multiphase systems. *AIChE J*. 2007;53:1941–1951.
17. Shi YF, Fan LT. Lateral mixing of solids in batch gas solids fluidized-beds. *Ind Eng Chem Process Des Dev*. 1984;23:337–341.
18. Berruti F, Scott DS, Rhodes E. Measuring and modelling lateral solid mixing in a three-dimensional batch gas-solid fluidized bed reactor. *Can J Chem Eng*. 1986;64:48–56.
19. Liu D, Chen X. Experimental profiles of lateral mixing of feed particles in a three-dimensional fluidized bed. *AIChE J*. 2010. Published online in Wiley Online Library: DOI: 10.1002/aic.12376
20. Xiang Q, Huang G, Ni M, Cen K, Tao T. Lateral dispersion of large coal particles in an industrial-scale fluidized bed combustor. In: Mustonen JP, Editor, *Proceedings of the 9th International Conference on FBC*. Boston, MA: ASME, 1987:546–553.
21. Shen L, Xiao J, Niklasson F, Johnsson F. Biomass mixing in a fluidized bed biomass gasifier for hydrogen production. *Chem Eng Sci*. 2007;62:636–643.
22. Zhang Y, Jin B, Zhong W. Experiment on particle mixing in flat-bottom spout-fluid bed. *Chem Eng Process: Process Intens*. 2009;48:126–134.
23. Valenzuela JA, Glicksman LR. An experimental study of solids mixing in a freely bubbling two-dimensional fluidized bed. *Powder Technol*. 1984;38:63–72.
24. Glicksman L, Carr E, Noymer P. Particle injection and mixing experiments in a one-quarter scale model bubbling fluidized bed. *Powder Technol*. 2008;180:284–288.
25. Bellgardt D, Werther J. A novel method for the investigation of particle mixing in gas-solid systems. *Powder Technol*. 1986;48:173–180.
26. Schlichthaerle P, Werther J. Solids mixing in the bottom zone of a circulating fluidized bed. *Powder Technol*. 2001;120:21–33.
27. Chirone R, Miccio F, Scala F. On the relevance of axial and transversal fuel segregation during the FB combustion of a biomass. *Energy Fuels*. 2004;18:1108–1117.
28. Winaya INS, Shimizu T, Yamada D. A new method to evaluate horizontal solid dispersion in a bubbling fluidized bed. *Powder Technol*. 2007;178:173–178.
29. Holland DJ, Muler CR, Davidson JF, Dennis JS, Gladden LF, Hayhurst AN, Mantle MD, Sederman AJ. Time-of-flight variant to image mixing of granular media in a 3D fluidized bed. *J Magn Reson*. 2007;187:199–204.
30. Dechsiri C, Van der Zwan EA, Dehling HG, Hoffmann AC. Dispersion of particle pulses in fluidized beds measured by positron emission tomography. *AIChE J*. 2005;51:791–801.
31. Valenzuela JA, Glicksman LR. An experimental-study of solids mixing in a freely bubbling two-dimensional fluidized-bed. *Powder Technol*. 1984;38:63–72.
32. Borodulya VA, Epanov YG, Teplitskii YS. Horizontal particle mixing in a free fluidized bed. *J Eng Phys Thermophys*. 1982;42:528–533.
33. Salam TF, Ren Y, Gibbs BM. Lateral solid and thermal dispersion in fluidized bed combustors. In: *Proceedings of the 9th International Conference on FBC*. Boston, MA: ASME, 1987:541–545.
34. Shen LH, Zhang MY. Effect of particle size on solids mixing in bubbling fluidized beds. *Powder Technol*. 1998;97:170–177.
35. Yang HR, Lu JF, Liu Q, Yue GX. Lateral solids mixing in the dense zone of a circulating fluidized bed. *Chin J Chem Eng*. 2002;10:490–493.
36. Scott SA, Davidson JF, Dennis JS, Hayhurst AN. Heat transfer to a single sphere immersed in beds of particles supplied by gas at rates above and below minimum fluidization. *Ind Eng Chem Res*. 2004;43:5632–5644.
37. Ferziger JH, Peric M. *Computational Methods for Fluid Dynamics*, 3rd. Berlin: Springer-Verlag, 2002.

Manuscript received Sept. 1, 2010, revision received Feb. 1, 2011, and final revision received Mar. 15, 2011.